Structural Characteristics of the Cavern at a Fine Bubbled Stage of Cavitation

Nodirakhon Akramovna Usmonova
Assistant, Fergana Polytechnic Institute, Fergana

ABSTRACT

The article deals with shock pulses arising from the closure of bubbles, depending on the structure of the cavitation cavity. Since a fine-bubble stage of cavitation is usually observed on the elements of hydraulic structures, the structural characteristics of the three stages of the appearance of cavitation are further investigated. Studies of the structure of cavitation require the fixation of the spatial pattern of the bubble zone. This is due to the need to use a high intensity luminous flux with ultrashort exposure. To solve these problems, the holography method with the use of a ruby laser was applied.

KEYWORDS: *shock impulses, cavitation cavity, bubble zone, cavitation bubbles, velocity.*

The shock impulses are rising from the closure of the bubbles depend on the structure of the cavitation cavity. Since a fine-bubble stage of cavitation is usually observed on the elements of hydraulic structures, in the future we will talk about the structural characteristics of this stage.

Studies of the structure of cavitation require fixing the spatial pattern of the bubble zone. This is due to the need to use a high intensity luminous flux with ultrashort exposure. To solve these problems, the method of holography with the use of a ruby laser was applied. Hydrodynamic cavitation was excited in a chamber of rectangular cross-section $a \times b = 6 \times 80 мм$ behind a two-dimensional streamlined cylinder 35 mm in diameter (Fig. 2). A cavitation hydrotube with closed water circulation made it possible to independently change the flow rate and pressure. The range of relative stages of cavitation was within $\frac{K}{K_{кр}} = 0{,}82 - 0{,}4$ the flow rate in the compressed section $\vartheta_{сж} = 14 - 33 \frac{м}{сек}$.[1,2].

The holographic object - a cylindrical area of a cavitation plume with a diameter of 18 and a height of 6 mm, equal to the distance between the transparent walls of the cavitation chamber (Fig. 1), was illuminated by a laser beam.

The investigations used a УИГ -1М holographic setup with two lasers: a pulsed ruby laser for recording holograms and an ЛГ -36 continuous helium-neon laser for image reproduction and optical system alignment. The duration of a ruby laser pulse in the Q-switched mode using a passive shutter (a solution of cryptocyanin in ethanol) was 30 ns. The pulse of radiation energy in one mode is equal to 25 MJ. Such a combination of the radiation energy of the luminous flux and the exposure time makes it possible to obtain high-quality holograms of rapidly moving structural units of the cavitation zone [2-4]. Due to the periodic change in the pressure field in the upper and lower parts of the vortex wake, the number of bubbles in any region of the cavitation plume also periodically changes from a minimum to a maximum value. In order to be able to analyze the change in the structural data of the cavitation zone from its stage and flow rate, holograms are recorded in standby mode while synchronizing the operation of an optical quantum generator with an inductive pressure pulsation converter DD-10. Synchronization at the initial stages of cavitation $\frac{K}{K_{кр}} = 0,8 - 0,6$ carried out at the peak of negative polarity (with the largest bubble size), at advanced stages of cavitation $\frac{K}{K_{кр}} = 0,6 - 0,4$ - at the peak of positive polarity (with the smallest bubble size).

The image of the bubbles are holographic, transferred to the area in front of the hologram and magnified 5 times using the Jupiter-9 lens. The direct light beam is filtered by a point screen at the focus of the objective (Fig. 1). Cavitation bubbles in the reconstructed image are measured with a horizontal measuring microscope in 8-10 regions in three mutually perpendicular directions. The total increase in bubbles are 40-180 *. The preliminary calibration established a connection between the coordinates of the camera and the reconstructed image (a distance of 6 mm in the camera corresponds to 130 mm in the reconstructed image). In this case, the shape, size, and number of bubbles were recorded in a cylindrical volume 2-4 mm in diameter (which depends on the magnification).

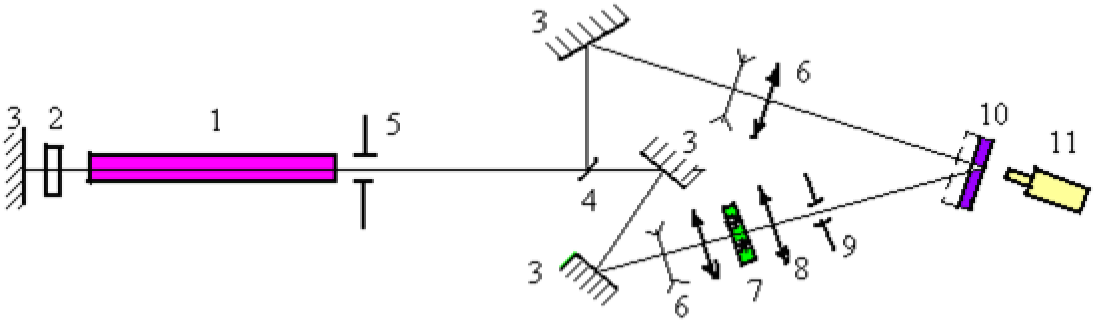

Fig. 1. Two-beam optical scheme of a holographic device for registering the structure of the cavitation zone. 1- single-mode ruby laser; 2- passive Q-switch; 3- mirror; 4- translucent mirror; 5- diaphragm; 6- collimator; 7- cavitation chamber; 8- photo lens; 9- wire diaphragm; 10- photographic plate (hologram); 11- measuring microscope.

Figure 1. the typical flat photographs of holographic images of both ensembles and individual bubbles, which do not give a figurative spatial picture of an object, obtained when examining a hologram with a microscope, are shown. Note that in these flat images, only bubbles with well-defined boundaries, i.e., those in focus, should be taken into account.

The holographic research method allows one to obtain the following characteristics: the concentration of bubbles, the distance between them, the shape of the bubbles, their average diameter, the voidness of the cavitating liquid

$$S = \frac{\sum V_П}{\sum (V_П + V_c)}$$

(the ratio of the total volume of bubbles to the volume of the two-phase mixture), the diagrams of the distribution of bubbles along the width of the chamber, etc. The recalculation of the area of the projection of the bubble into the volume is carried out using a generalized conversion factor with an accuracy of at least ± 2.7% according to the formula $V_П = \frac{(F_П)^{\frac{3}{2}}}{K}$, which is applicable provided that the bubble is a convex body, and the visible part of its surface repeats the invisible one. Table

4.3 shows the experimentally obtained structural characteristics of three stages of cavitation at a constant flow rate $\vartheta_{см} = 32{,}5\frac{м}{с}$ .Almost 160 bubbles were processed for each stage. It should be noted that at the initial stages of cavitation, the overwhelming majority of small spherical bubbles with a diameter of less than 0.1 mm are observed. With the development of cavitation, the voidness and the average diameter of the bubbles increase (Fig. 1), and the percentage of the content of nonspherical cavitation bubbles also increases.

Table 1. Structural characteristics of the fine-bubble stage of cavitation

Structural characteristic	Cavitation mode		
	$\beta = \frac{K}{K_{кр}} = 0{,}82(\lambda = 0{,}5)$	$\beta = 0{,}725(\lambda = 1)$	$\beta = 0{,}685(\lambda = 1{,}5)$
Average radius r mm	0,015	0,02	0,03
Emptiness 5	$2{,}3 \cdot 10^{-4}$	$8{,}9 \cdot 10^{-4}$	$3{,}7 \cdot 10^{-3}$
Bubble concentration, pcs, / mm^3	7,2	9,5	13
Average distance between bubbles a mm	0,48	0,42	0,34
Relative distance between bubbles a/r	25	15	8
Bubble fraction $\frac{r \succ 0{,}05мм}{r \succ 0{,}05мм}$ %	45/95,5	5/95	18/92
Including non-spherical ,%	100/5,5	100/8,5	66/7

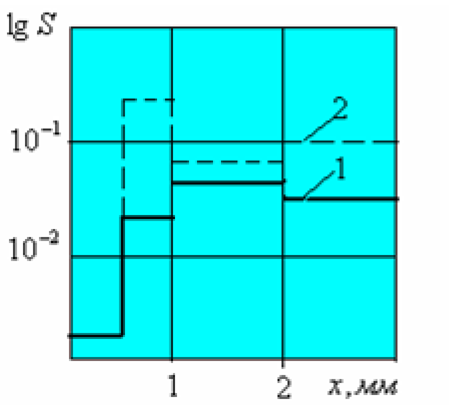

Fig. 2. Diagram of changes in the cavitation zone emptiness S depending on the distance *K* from the chamber wall

The form of the distribution density functions of the radii of cavitation bubbles fixed in the cylindrical region 4 from the wall to the wall of the working chamber (see Fig. 2) indicates that the sizes of cavitation bubbles vary within limited limits from $r_{мин} \succ 0$ before $r_{макс} \prec 1мм$ (fig. 2).

In this graph, the left part of the curves are drawn conditionally, since the quality of the used optical equipment and photomaterial does not allow fixing the clear outlines of bubbles with a radius $r \prec 0{,}008мм$. The probability of detecting a bubble of a given size when its radius decreases from $r_{мин}$ first increases from 0 (at $r_{макс}$) to the maximum value, and then decreases again to 0 (at $r_{мин}$). Distribution histograms have a pronounced asymmetry, and the modal value of the radius r_0 shifted to the left relative to the central value (mathematical expectation of the radius $\bar{r}$). These distributions can be approximated logarithmically - by the normal law, as is usually accepted when describing the distribution of individuals in two-phase media;

$$f(r)=\frac{A}{r}\varphi(t) \qquad (1)$$

Where $\varphi(t)=\sqrt{\frac{1}{2\pi}}e^{-\frac{t^2}{2}}$; and $t=\frac{\lg r-\lg\bar{r}}{D_{\lg r}}$ — mathematical expectation and variance of the quantity, $\lg r$ respectively. The density functions of the probability distribution of bubble radii (Fig. 2), referred to 1 cm^3, have the following analytical expressions:

$$\left.\begin{array}{l}
при \beta=\frac{K}{K_{кр}}=0{,}82\left(\lambda=\frac{l}{d}=0{,}5\right) \\
f(r)=\frac{12{,}8\times10^3}{r}\frac{1}{\sqrt{2\pi}}\exp\left[-\frac{\left(\frac{\lg r+2{,}83}{0{,}245}\right)^2}{2}\right] \\
при \beta=0{,}725(\lambda=1) \\
f(r)=\frac{12{,}8\times10^3}{r}\frac{1}{\sqrt{2\pi}}\exp\left[-\frac{\left(\frac{\lg r+2{,}72}{0{,}283}\right)^2}{2}\right]; \\
при \beta=0{,}685(\lambda=1{,}5) \\
f(r)=\frac{20{,}8\times10^3}{r}\frac{1}{\sqrt{2\pi}}\exp\left[-\frac{\left(\frac{\lg r+2{,}52}{0{,}272}\right)^2}{2}\right].
\end{array}\right\} \qquad (2)$$

The data presented show that when the stages of cavitation change from the initial $\beta=0{,}82$ to more developed $\beta=0{,}685$ average bubble size increases. In this case, the probability of the appearance of bubbles with a radius $r=0{,}01мм$ about 3 times higher at $\beta=0{,}82$, than with $\beta=0{,}685$. However, the likelihood of bubbles $r=0{,}03мм$ 3 times lower for $\beta=0{,}82$, than with $\beta=0{,}685$ (fig. 2). The percentage of non-spherical bubbles increases sharply in this case (see Table 1).

Flow rate at $\beta=const$ also significantly affects the structural characteristics of the cavitation plume. For example, with an increase in the flow rate from $\vartheta_н=13{,}7$ before 26,7 м/с at $\beta=0{,}725=const$.

The average radius of the bubbles approximately doubled, and the voidness decreased by 4-6 times.

The bubble concentration and voidness over the chamber width remained practically constant, with the exception of the near-wall layer 0.5 mm thick, in which the value decreased by an order of magnitude in all modes. Thus, in the zone of the near vortex wake behind the cavitation exciter, where intense turbulent mixing occurs, the bubble concentration diagram over the flow cross section is practically rectangular.

The given structural parameters characterize the cavitating liquid as a quasi-homogeneous medium and do not give an idea of the macrostructural inhomogeneities in the cavitation plume observed in the reconstructed image. On some holograms, garlands up to 16 mm long are recorded from bubbles 0.1–0.3 mm in size, located in one layer close to each other or at a distance of up to 0.02 mm. Such inhomogeneities are mainly concentrated at the axis of vortices descending from the streamlined body, which suggests their weak effect on cavitation fractures [1,3,5].

Conclusions: To study the kinematics of the bubble near the wall, the ruby laser operated in the free-running mode under pumping with a total radiation pulse duration of up to 500 μs. This duration allows using a passive shutter to obtain up to three short light pulses (30-40 ns) of modulated Q-switch. Time intervals between pulses are measured on the screen of a storage oscilloscope and are 20-100 μs. The transmission of a light pulse to the oscilloscope is carried out by a coaxial photocell 30 ФЭК -09.

The data obtained showed that the cavitation bubble approaches the wall at a speed of 10–30 m / s and at the same time it decreases in volume by a factor of 4–10. The trajectory of the "settling" of the bubble on the wall is a winding line.

References

1. Амромин Э. Л., Иванов А. Н. Осесимметричное кавитационное обтекание тела в трубе.- Там же, 1976, № 4, с. 50-55.
2. Балуев Е. Д., Троянкин Ю. В. Исследование аэродинамической структуры газового потока в циклонной камере.— Теплоэнергетика, 1967, № 1, с. 18-20.
3. Башарова В. Н.Пространственные кавитационные течения за произвольно ориентированными некруговыми кавитаторами.— В кн.: Математические методы исследования гидродинамических течений : Сб. науч. тр. Киев : Наук, думка, 1978,с. 41-45.
4. Хамидов А.А. Плоские и осесимметрические задачи о струйном течении идеальной сжимаемой жидкости. Ташкент: Фан, 1978.
5. Хамидов А.А.,Худайкулов С.И. Теория струй смеси вязких жидкостей. Ташкент: Фан, 2003.
6. Xamdamaliyevich, Sattorov Alimardon, and Salimjon Azamdjanovich Rahmankulov. "INVESTIGATION OF HEAT TRANSFER PROCESSES OF SOLAR WATER, AIR CONTACT COLLECTOR." In *E-Conference Globe*, pp. 161-165. 2021.
7. M.M.Madraximov, Z.E.Abdulxayev, E.M.Yunusaliev, A.A.Akramov. “Suyuqlik Va Gaz Mexanikasi Fanidan Masalalar To’plami” Oliy o‘quv yurtlari talabalari uchun o‘quv qo‘llanma. - Farg’ona: 2020-yil, 232 bet.
8. ABDULKHAEV, ZOKHIDJON ERKINJONOVICH. "Protection of Fergana City from Groundwater." *Euro Afro Studies International Journal* 6 (2021): 70-81.
9. Абдукаримов, Бекзод Абобакирович, Ахрор Адхамжон Угли Акрамов, and Шахноза Бахтиёрбек Кизи Абдухалилова. "Исследование повышения коэффициента полезного действия солнечных воздухонагревателей." *Достижения науки и образования* 2 (43) (2019).

10. Рашидов, Ю. К., Ж. Т. Орзиматов, and М. М. Исмоилов. "Воздушные солнечные коллекторы: перспективы применения в условиях Узбекистана." In *Экологическая, промышленная и энергетическая безопасность-2019*, pp. 1388-1390. 2019.
11. Bekzod, Abdukarimov. "Relevance of use of solar energy and optimization of operating parameters of new solar heaters for effective use of solar energy." *IJAR* 6, no. 6 (2020): 16-20.
12. Malikov, Zafar Mamatkulovich, and Murodil Erkinjanovich Madaliev. "Mathematical modeling of a turbulent flow in a centrifugal separator." *Vestnik Tomskogo Gosudarstvennogo Universiteta. Matematika i Mekhanika* 71 (2021): 121-138.
13. Mirsaidov, Mirziyod, Abdurasul Nosirov, and Ismoil Nasirov. "Spatial forced oscillations of axisymmetric inhomogeneous systems." In *E3S Web of Conferences*, vol. 164, p. 02009. EDP Sciences, 2020.
14. Abobakirovich, Abdukarimov Bekzod, O'Gli Mo'Minov Oybek Alisher, and Shoyev Mardonjon Ahmadjon O'G'Li. "Calculation of the thermal performance of a flat solar air heater." *Достижения науки и образования* 12 (53) (2019).
15. Akhmadaliev, M. A., R. M. Mat'yakubov, N. A. Sal'nikova, E. U. Madaliev, and P. CURTIS. "SYNTHESIS AND PROPERTIES OF TETRAFURFURYL TITANATE." *International polymer science and technology* 23, no. 1 (1996): 34-35.
16. Erkinjonovich, Abdulkhaev Zokhidjon, and Madraximov Mamadali Mamadaliyevich. "WATER CONSUMPTION CONTROL CALCULATION IN HYDRAULIC RAM DEVICE." In *E-Conference Globe*, pp. 119-122. 2021.
17. Abdukarimov, B. A., Sh R. O'tbosarov, and M. M. Tursunaliyev. "Increasing Performance Efficiency by Investigating the Surface of the Solar Air Heater Collector." *NM Safarov and A. Alinazarov. Use of environmentally friendly energy sources* (2014).
18. Usarov, M., G. Ayubov, G. Mamatisaev, and B. Normuminov. "Building oscillations based on a plate model." In *IOP Conference Series: Materials Science and Engineering*, vol. 883, no. 1, p. 012211. IOP Publishing, 2020.
19. Мадрахимов, М. М., З. Э. Абдулҳаев, and Н. Э. Ташпулатов. "Фарғона Шаҳар Ер Ости Сизот Сувлари Сатҳини Пасайтириш." *Фарғона Политехника Институти Илмий–Техника Журнали* 23, no. 1 (2019): 54-58.
20. Abdulkhaev, Zokhidjon, Mamadali Madraximov, Axmadullo Abdurazaqov, and Mardon Shoyev. "Heat Calculations of Water Cooling Tower." *Uzbekistan Journal of Engineering and Technology* (2021).
21. Abdukarimov, Bekzod, Shuhratjon O'tbosarov, and Axmadullo Abdurazakov. "Investigation of the use of new solar air heaters for drying agricultural products." In *E3S Web of Conferences*, vol. 264, p. 01031. EDP Sciences, 2021.
22. Abdulkhaev, Zokhidjon Erkinjonovich, Axmadullo Muxammadovich Abdurazaqov, and Abdusalom Mutalipovich Sattorov. "Calculation of the Transition Processes in the Pressurized Water Pipes at the Start of the Pump Unit." *JournalNX* 7, no. 05: 285-291.
23. Xamdamaliyevich, Sattorov Alimardon, and Salimjon Azamdjanovich Rahmankulov. "INVESTIGATION OF HEAT TRANSFER PROCESSES OF SOLAR WATER, AIR CONTACT COLLECTOR." In *E-Conference Globe*, pp. 161-165. 2021.

24. Мадхадимов, М. М., Абдулхаев, З. Э., & Сатторов, А. Х. (2018). Регулирования работы центробежных насосов с изменением частота вращения. *Актуальные научные исследования в современном мире*, (12-1), 83-88.
25. Абдукаримов, Б. А., О. А. Муминов, and Ш. Р. Утбосаров. "Оптимизация рабочих параметров плоского солнечного воздушного обогревателя." In *Приоритетные направления инновационной деятельности в промышленности*, pp. 8-11. 2020.
26. Erkinjonovich, Abdulkhaev Zokhidjon, Madraximov Mamadali Mamadaliyevich, Shoev Mardonbek Axmadjon O'G'Li, and Toshpulatov Nosirbek Egamberdiyevich. "FARG'ONA SHAHAR YER OSTI SIZOT SUVLARINING KO'TARILISH MUAMMOSI VA YECHIMLARI." *Oriental renaissance: Innovative, educational, natural and social sciences* 1, no. 3 (2021): 138-144.
27. Усаров, М. К., and Г. И. Маматисаев. "Свободные колебания коробчатой конструкции здания." *Проблемы механики.* 5-6 (2009): 31.
28. Mirsaidov, M. M., A. A. Nosirov, and I. A. Nasirov. "Modeling of spatial natural oscillations of axisymmetric systems." In *Journal of Physics: Conference Series*, vol. 1921, no. 1, p. 012098. IOP Publishing, 2021.
29. Маликов, З. М., and М. Э. Мадалиев. "Численное моделирование течения в плоском внезапно расширяющемся канале на основе новой двужидкостной модели турбулентности." *Вестник Московского государственного технического университета им. НЭ Баумана. Серия Естественные науки* 4 (2021): 24-39.
30. Рашидов, Ю. К., М. М. Исмоилов, Ж. Т. Орзиматов, К. Ю. Рашидов, and Ш. Ш. Каршиев. "Повышение эффективности плоских солнечных коллекторов в системах теплоснабжения путём оптимизации их режимных параметров." In *Экологическая, промышленная и энергетическая безопасность-2019*, pp. 1366-1371. 2019.
31. Абдулхаев, Зохиджон Эркинжонович, and Абдусалом Муталипович Сатторов. "CENTRAL PUMP CASE ADJUSTMENT BY CHANGING THE ROTATION FREQUENCY." *Актуальные научные исследования в современном мире* 6-1 (2020): 20-25.